

THz lasing in a polariton system: Quantum theory

Elena del Valle and Alexey Kavokin

School of Physics and Astronomy, University of Southampton, SO17 1BJ, Southampton, United Kingdom

(Dated: August 23, 2021)

We study the laser regime of terahertz (THz) emission from a semiconductor microcavity in the strong coupling regime, where optical transitions between upper and lower exciton-polariton modes are allowed due to the mixing of the upper mode with one of the dark exciton states. Using a system of master-Boltzmann equations describing both polariton modes and the THz mode, we calculate the first and second order coherences and the spectral shape of THz emission. This analysis shows that THz lasing in microcavities is possible provided that the system is embedded in a good THz cavity, that the optical (polariton) lasing condition is fulfilled and if the depletion of the upper polariton mode due to acoustic phonon assisted relaxation processes is reduced. This latter condition is likely to be realised in pillar microcavities, which seem to be the most suitable candidates for realisation of a THz laser.

Realisation of efficient terahertz (THz) radiation sources and detectors is one of the important objectives of modern applied optics [1, 2]. THz radiation based methods have a lot of potential applications in biology, medicine, security and non-destructive in-depth imaging. Also, wireless data transfer utilising THz radiation could provide higher transfer rates for in-door short distance or high altitude communications.

To allow such applications of THz radiation, the creation of cheap, reliable, scalable and portable emitters is extremely important. None of the existing ones so far satisfies all the application requirements. For example, the emitters based on nonlinear-optical frequency down-conversion, gas THz laser, vacuum tube and systems based on short-pulse spectroscopy are bulky, expensive, and power consuming. Various semiconductor devices based on intersubband optical transitions [3] are compact but have a limited wavelength adjustment range, have low quantum efficiency and require cryogenic cooling. Among the factors which limit the efficiency of semiconductor THz sources is the short lifetime of the electronic states involved (typically, fractions of a nanosecond) compared to the time for spontaneous emission of a THz photon (typically milliseconds). The methods of reducing this mismatch include the use of the Purcell effect in THz cavities or the cascade effect in quantum cascade lasers [4–6] (QCL). Nevertheless, till now the QCL in the spectral region about 1THz remains costly and short-lived and still show a quantum efficiency of less than 1%. Moreover, so far there are no commercially available reliable compact and cheap detectors of THz radiation which are in great need for information communication technologies.

Recent studies of strong coupling intersubband microcavities have shown the possibility of stimulated scattering of intersubband polaritons [7]. Very recently, it was proposed to generate THz radiation in semiconductor microcavities in the regime of exciton-polariton lasing [8]. The quantum efficiency of this THz source is governed by population of the final polariton state, which may be tuned over a large range by means of the optical pumping. In the strong coupling regime in a microcavity [9], the dispersion of exciton-polaritons is described by two bands both having minima at zero in-plane wave vector k . At $k = 0$, the energy splitting between the two branches is of the order of several meV, which makes this system attractive for THz applications (1THz corresponds to

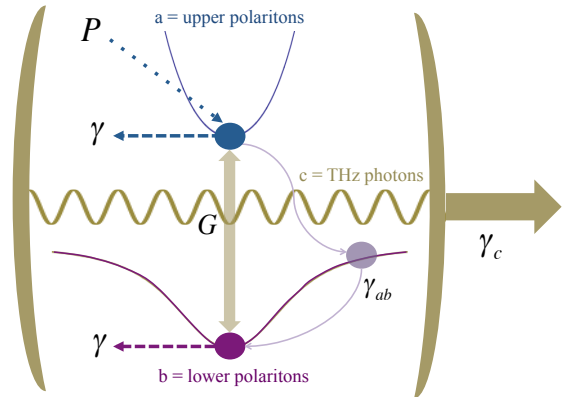


FIG. 1. Scheme for the THz laser in a microcavity embedded in a THz cavity. Upper and lower polariton branches (dispersion relation) are depicted in blue and pink, respectively, with the mechanisms considered for all the modes (a , b , c): decay (γ , γ_c), non-resonant continuous pump (electronic injection) on the upper branch (P) and upper to lower polariton relaxation via exciton reservoir (γ_{ab}). THz photons are emitted (absorbed) during the upper to lower (lower to upper) polariton conversion at rate G .

4meV). Stimulated scattering of exciton polaritons into the lowest energy state leads to so-called polariton lasing, recently observed in GaAs [10] and GaN [11] based microcavities. If the scattering from the upper to the lower polariton branch were accompanied by the emission a photon, polariton lasers would emit THz radiation, and this emission would be stimulated by the population of the lowest energy polariton state. However, this process is a priori forbidden since an optical dipole operator cannot directly couple the polariton states formed by the same exciton state. This obstacle can be removed if one of the polariton states of interest is mixed with an exciton state of a different parity, say, the $e1hh2$ exciton state formed by an electron at the lowest energy level in a quantum well (QW) and a heavy hole at the second energy level in the QW [8]. This state is typically a few meV above the exciton ground state, $e1hh1$. Nevertheless, by an appropriate choice of the QW width and exciton-photon detuning in the microcavity, the state can be brought into resonance with the lowest

energy upper polariton state. Being resonant, the two states can be easily hybridised by any weak perturbation, such as, e.g., a built-in or applied electric field. The optical transition between such a hybridised state and the lowest ehh1 exciton polariton state is allowed.

In this Letter, we describe theoretically the quantum properties of THz light generated by polariton lasers according to the above scheme. We consider the model system shown in Fig. 1. It consists of a microcavity with embedded quantum wells operating in the strong coupling regime, and placed inside a THz cavity. Together with the wave-guiding effect of the microcavity structure, adding the lateral THz cavity would achieve an effective 3D confinement of the THz mode, giving rise to enhancement of spontaneous emission rate through the Purcell effect [12–14]. We will show that in the polariton lasing regime, this device also operates as a THz laser. Moreover, polariton lasing may be triggered by an external THz radiation which would stimulate scattering of polaritons between the upper and lower modes in the microcavity. Therefore, the proposed device could also operate as a detector of THz radiation.

The two polariton branches at $k = 0$ are modelled by two Bose fields with annihilation operators a (upper) and b (lower). Both modes (being at resonance) lose particles at the same rate γ . This rate provides the units of the problem (for standard microcavities, $\gamma \approx 0.1\text{ps}^{-1}$). In Fig. 1, the system is sketched together with the relevant parameters. Only one of the modes, a , receives incoherently polaritons at a rate P due to electronic injection. Upper polaritons can convert into lower polaritons by emitting a THz photon (with operator c) at a rate G . Energy is conserved in this process as $E_c = E_a - E_b$. The opposite process happens with the same probability G since the THz photons, once emitted, remain in the cavity long enough to make the transformation reversible. The THz cavity is not perfect and does, however, lose particles at a rate γ_c . There is a last relaxation process that must be included: the conversion of upper polaritons into lower ones via the exciton reservoir at rate γ_{ab} , through irreversible phonon emission. This process is important in planar microcavities and is unfavorable for THz generation, as will be shown below. Fortunately, the acoustic phonon induced depletion of the upper polariton mode may be strongly suppressed in micropillars [10]. All these incoherent processes can be described as Lindblad terms (\mathcal{L}) in the master equation of the total density matrix of the system, ρ :

$$\partial_t \rho = \left[\frac{\gamma}{2} (\mathcal{L}_a + \mathcal{L}_b) + \frac{\gamma_c}{2} \mathcal{L}_c + \frac{P}{2} \mathcal{L}_{a^\dagger} + \frac{\gamma_{ab}}{2} \mathcal{L}_{(ab^\dagger)} \right] \rho \quad (1a)$$

$$+ \frac{G}{2} (\mathcal{L}_{(ab^\dagger c^\dagger)} + \mathcal{L}_{(a^\dagger bc)}) \rho, \quad (1b)$$

where $\mathcal{L}_O \rho \equiv 2O\rho O^\dagger - O^\dagger O\rho - \rho O^\dagger O$. All the irreversible processes are gathered in Eq. (1a), that is, decay, non-resonant pump and relaxation processes. Eq. (1b) represents the non-linear processes of upper to lower polariton conversion and THz photon emission (and vice versa) similarly to the evaporative cooling processes in an atom laser [15–17].

The Hilbert space of the three modes is spanned by the number states $\{|n, m, r\rangle$ with $n, m, r \in \mathbb{N}\}$ the number of upper

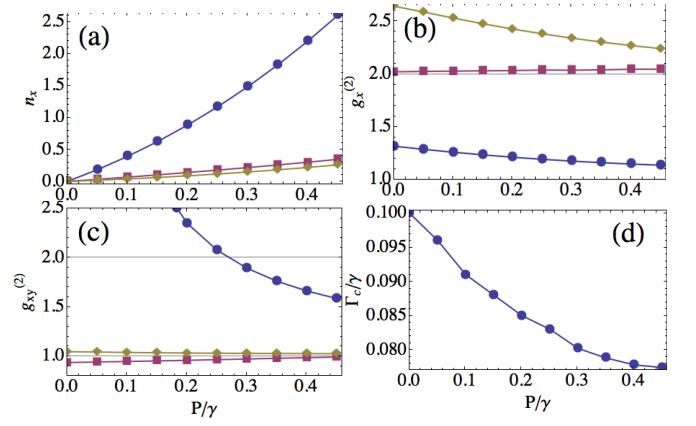


FIG. 2. Relevant quantities in the steady state as a function of pump, for the THz field ($x = c$ in blue, circles), the upper polaritons ($x = a$, in purple, squares) and the lower polaritons ($x = b$ in brown, rhombus). (a) Average populations n_x . (b) Second order coherence functions $g_x^{(2)}$. (c) Cross correlation functions $g_{bc}^{(2)}$, $g_{ac}^{(2)}$ and $g_{ab}^{(2)}$. (d) Linewidth of the THz spectrum of emission. Parameters are: $G = \gamma$, $\gamma_{ab} = 0$ and $\gamma_c = 0.1\gamma$.

polaritons, lower polaritons and THz photons, respectively. The occupation of these states described by the probability function $\mathcal{P}_{[n,m,r]} \equiv \langle n, m, r | \rho | n, m, r \rangle$ follows the set of coupled quantum Boltzmann master equations [18]:

$$\begin{aligned} \partial_t \mathcal{P}_{[n,m,r]} = & - \left\{ \gamma(n+m) + \gamma_c r + P(n+1) \right\} \mathcal{P}_{[n,m,r]} \\ & + \gamma \left\{ (n+1) \mathcal{P}_{[n+1,m,r]} + (m+1) \mathcal{P}_{[n,m+1,r]} \right\} \\ & + \gamma_c (r+1) \mathcal{P}_{[n,m,r+1]} + Pn \mathcal{P}_{[n-1,m,r]} \\ & + \gamma_{ab} \left\{ (n+1)m \mathcal{P}_{[n+1,m-1,r]} - n(m+1) \mathcal{P}_{[n,m,r]} \right\} \\ & + G(n+1)mr \left\{ \mathcal{P}_{[n+1,m-1,r-1]} - \mathcal{P}_{[n,m,r]} \right\} \\ & + Gn(m+1)(r+1) \left\{ \mathcal{P}_{[n-1,m+1,r+1]} - \mathcal{P}_{[n,m,r]} \right\}. \quad (2) \end{aligned}$$

In what follows, we solve these equations numerically in the steady state of the system. Then, any average single-time quantity can be computed as $\langle O \rangle = \text{Tr}(\rho O) = \sum_{n,m,r} \mathcal{P}_{[n,m,r]} \langle n, m, r | O | n, m, r \rangle$. The relevant quantities characterizing each mode ($x = a, b, c$), that we use to study lasing emission and correlations are: the average occupation numbers $n_x = \langle x^\dagger x \rangle$; the second order temporal correlation function at zero delay, $g_x^{(2)} = \langle x^\dagger x^\dagger x x \rangle / n_x^2$, that is 2 for a thermal and 1 for a Poissonian distribution; the cross correlation function between two modes x and y , $g_{xy}^{(2)} = \langle x^\dagger x y^\dagger y \rangle / (n_x n_y)$. These quantities are plotted in Fig. 2(a,b,c) as a function of the pumping rate P . Let us explain the choice of parameters of this figure, that brings the system in the THz lasing regime.

The first condition for THz lasing is the accumulation of a large population of THz photons ($n_c \gg 1$), for which a strong nonlinearity and a good THz cavity are required. Furthermore, this should also lead to a coherence buildup ($g_c^{(2)} \rightarrow 1$). Assuming that other destructive issues (as pure dephasing)

are negligible in the system, the efficiency of such coherence buildup is further enhanced by the irreversibility of the polariton-to-photon conversion [17]. The conversion should happen effectively mainly in the polariton-to-photon sense so that the formation of correlations is not disrupted by the inverse process. However, if, after one upper polariton has transformed into a THz photon plus a lower polariton, these two last remain for a long time in the cavity, the inverse process is more likely to happen. Given that, at the same time, we wish the THz population to remain high, the only way to suppress the photon-to-polariton process is that lower polaritons do not remain for long times in the cavity, that is, we need $\gamma \gg \gamma_c$. Therefore, we have chosen $G = \gamma$ and $\gamma_c = 0.1\gamma$, which allows for an accumulation of photons faster than of polaritons, as shown in Fig. 2(a). For the moment, we have also neglected the competing process through the exciton reservoir ($\gamma_{ab} = 0$) that does not produce THz radiation and clearly hinders lasing. In these conditions, Fig. 2(a) shows a nonlinear increase of the THz population (circles) which is accompanied by the expected $g_c^{(2)} \rightarrow 1$ in Fig. 2(b). Note that there is not a sharp threshold for the lasing emission. The THz photons gradually and monotonously increase and acquire coherence. One can in any case define the threshold as the pump where $n_c = 1$, that is, $P \approx 0.22\gamma$ in this case.

To link the present full-quantum master equation approach with the kinetic model [8], we derive from Eq. (1) the steady state equations for the average populations, that are of the type of a Boltzmann source and sink rate equation, i.e.,

$$n_x = P_x^{\text{eff}} / \Gamma_x^{\text{eff}} \quad (3)$$

for $x = a, b, c$. This provides us with the effective pumping and intensity decay rates for the three modes:

$$P_a^{\text{eff}} = P + Gg_{bc}^{(2)}n_b n_c \quad (4a)$$

$$\Gamma_a^{\text{eff}} = \gamma - P + \gamma_{ab}(1 + g_{ab}^{(2)}n_b) + G(1 + g_{ab}^{(2)}n_b + g_{ac}^{(2)}n_c) \quad (4b)$$

$$P_b^{\text{eff}} = [\gamma_{ab} + G(1 + g_{ac}^{(2)}n_c)]n_a \quad (4c)$$

$$\Gamma_b^{\text{eff}} = \gamma - \gamma_{ab}g_{ab}^{(2)}n_a + G(g_{bc}^{(2)}n_c - g_{ab}^{(2)}n_a) \quad (4d)$$

$$P_c^{\text{eff}} = G(1 + g_{ab}^{(2)}n_b)n_a \quad (4e)$$

$$\Gamma_c^{\text{eff}} = \gamma_c + G(g_{bc}^{(2)}n_b - g_{ac}^{(2)}n_a). \quad (4f)$$

The semiclassical rate equations of Ref. [8] are recovered by setting all cross correlation functions to unity. Solving exactly these rate equations, one obtains approximated formulas for the populations that, in turn, provide analytical expressions for all the effective parameters above. The expressions are too lengthy to be given here but we still note them as n_x^{rate} , P_x^{rate} and Γ_x^{rate} for later comparison.

In our full quantum derivation, cross correlation functions are computed numerically and self-consistently and can be, in general, larger (resp. smaller) than unity, showing bunching (resp. antibunching) of joint emission in the modes x and y . This is shown in Fig. 2(c), where cross emission between upper polaritons and THz photons is antibunched (squares, $g_{ac}^{(2)} < 1$), as the destruction of the first one implies the creation of the second ones. This also tends to be the case between upper and lower polaritons, however, in this case due to

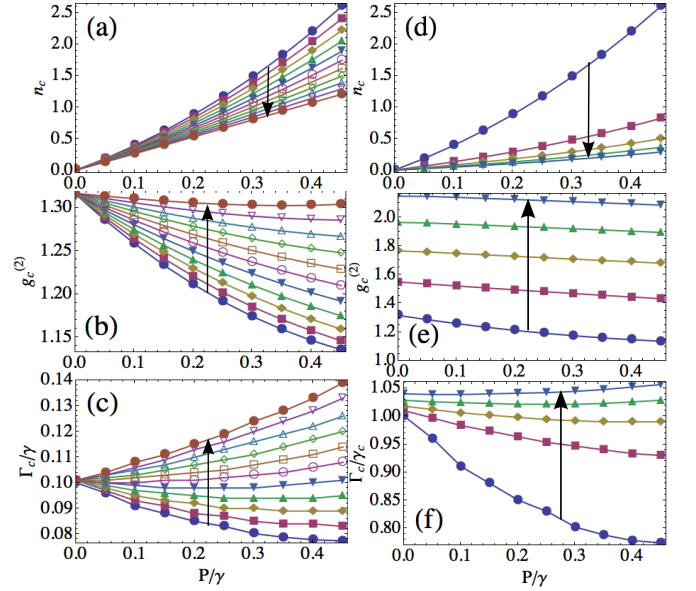


FIG. 3. Relevant THz quantities in the steady state as a function of pump: n_c (first line), $g_c^{(2)}$ (second line) and Γ_c (third line). The first column (plots a, b, c) corresponds to fixing $\gamma_c = 0.1\gamma$ and increasing γ_{ab} in the sense indicated by the arrow (from 0 to 0.5 in steps of 0.05). The second column (plots d, e, f) corresponds to fixing $\gamma_{ab} = 0$ and increasing γ_c in the sense indicated by the arrow (from 0.1 to 0.9 in steps of 0.1).

the large difference $n_b \ll n_c$, they have become independent (rhombus, $g_{ab}^{(2)} \approx 1$). The cross emission of lower polaritons and THz photons is bunched (circles, $g_{bc}^{(2)} > 1$) for the same reason: they are produced at the same time and their emission tends to be simultaneous. At very high pumps all the emissions become statistically independent ($g_{xy}^{(2)} \rightarrow 1$).

Another typical manifestation of lasing is line narrowing of the luminescence emission, that is, the increasing lifetime of the photons emitted by the lasing mode: in the incoherent regime, the linewidth corresponds to the inverse lifetime of a single (incoherent) photon, whereas in the lasing regime, THz photons form a collective state with a lifetime affected by the total population. The effective inverse lifetime of the THz mode is given approximately by Eq. (4f) in the limit of independent classical modes. Γ_c^{eff} decreases appreciably when G is large and $g_{bc}^{(2)}n_b - g_{ac}^{(2)}n_a$ decreases with pumping. In the case of Fig. 2, where $g_{ac}^{(2)} \approx 1$ and n_a, n_b are small, the main element that determines the linewidth is the cross correlation function $g_{bc}^{(2)}$, which is large (bunched) but strongly decreasing with pump.

To check that this process is accompanied by the expected line narrowing of the emission, predicted by Eq. (4f) in the regime of Fig. 2, we compute the photoluminescence spectrum of THz emission. It is defined, in the steady state, as $S(\omega) \propto \Re \int_0^\infty \langle c^\dagger(0)c(\tau) \rangle e^{i\omega\tau} d\tau$ and is computed (with the quantum regression formula) from the two-time correlator:

$$\langle c^\dagger(0)c(\tau) \rangle = \sum_{n,m,r} \sqrt{r} \mathcal{W}_{[n,m,r]}(\tau) \quad (5)$$

in terms of $\mathcal{W}_{[n,m,r]}$, that follow the same equation as the off-diagonal density matrix elements $\langle n, m, r | \rho | n, m, r-1 \rangle$, with initial values $\mathcal{W}_{[n,m,r]}(0) = \sqrt{r} \mathcal{P}_{[n,m,r]}$. The required equations read:

$$\begin{aligned} \partial_\tau \mathcal{W}_{[n,m,r]} = & - \left\{ \gamma(n+m) + \gamma_c \left(r - \frac{1}{2} \right) + P(n+1) \right\} \mathcal{W}_{[n,m,r]} \\ & + \gamma \left\{ (n+1) \mathcal{W}_{[n+1,m,r]} + (m+1) \mathcal{W}_{[n,m+1,r]} \right\} \\ & + \gamma_c \sqrt{r(r+1)} \mathcal{W}_{[n,m,r+1]} + Pn \mathcal{W}_{[n-1,m,r]} \\ & + \gamma_{ab} \left\{ (n+1)m \mathcal{W}_{[n+1,m-1,r-1]} - n(m+1) \mathcal{W}_{[n,m,r]} \right\} \\ & + G(n+1)m \left\{ \sqrt{r(r-1)} \mathcal{W}_{[n+1,m-1,r-1]} - \left(r - \frac{1}{2} \right) \mathcal{W}_{[n,m,r]} \right\} \\ & + Gn(m+1) \left\{ \sqrt{r(r+1)} \mathcal{W}_{[n-1,m+1,r+1]} - \left(r + \frac{1}{2} \right) \mathcal{W}_{[n,m,r]} \right\}. \end{aligned} \quad (6)$$

The THz spectrum of emission consists of only one peak. The associated linewidth is extracted and plotted in Fig. 2(d). We find that, although not quantitatively exact, the trend (narrowing) follows remarkably that predicted by the effective THz intensity decay rate, Eq. (4f).

Finally, in Fig. 3, we analyse how two key factors influence the quality of the THz lasing. Still as a function of pump, we show how THz population (first row), coherence $g_c^{(2)}$ (second row) and its spectral linewidth, Γ_c , (third row) are spoiled as, on the one hand, incoherent relaxation from upper to lower polaritons through the reservoirs (i.e., not through the THz mode) is increased (left column), and, on the other hand, as the THz cavity Q factor is decreased (right column). The sharpest feature to tell when lasing disappears is the slope of the linewidth curve, that becomes positive at all pumps. This happens at $\gamma_{ab} \approx 0.2\gamma$ in the first case and at $\gamma_c \approx 0.7\gamma$ in the second. These are the minimum values required to achieve the THz lasing with all its features. The analytical approximated expression for the linewidth, Γ_c^{rate} , is only valid for a bad THz cavity, when the system is in the “weak coupling regime” ($\gamma_c > G$, γ) with the THz mode (see Fig. 4). Here, the rate equations, that neglect quantum correlations, give a good description of the dynamics. With better systems able to enter the lasing regime, one must solve the full quantum problem, including one- and two-time correlators, in order to retain important qualitative features of the linewidth such as line narrowing.

To conclude, our analysis shows that although an efficient THz lasing is indeed possible in optically pumped polariton systems, it requires a special care in the design of the structure. One must ensure a good THz cavity and small depletion of the $k=0$ state of the upper polariton mode due to the phonon-assisted relaxation of polaritons from this state to the states of the lower polariton mode characterised by large in-plane wavevectors k . The latter obstacle is the most serious as upper polariton depletion is usually very fast in planar cavities. This can be circumvented by the use of pillar microcavities [10], where a full three-dimensional photonic confinement is achieved. In pillars, the spectrum of exciton-polaritons consists of discrete states, so that there is no reservoir of states

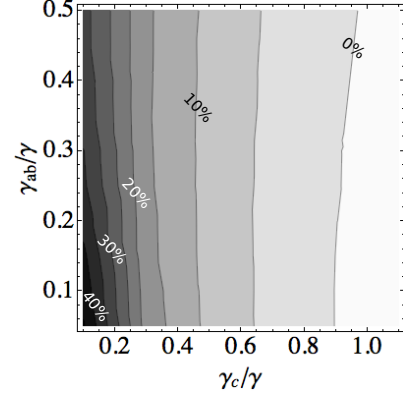


FIG. 4. Difference between the numerically computed THz emission linewidth (Fig. 3c,f) and the analytical approximated formula obtained from the rate equations: $100(\Gamma_c^{\text{rate}} - \Gamma_c)/\Gamma_c$. Pumping is fixed at $P = 0.451\gamma$.

with large wavevectors. Optical transitions between exciton polariton states in the pillars are usually forbidden, but if one of these states is brought into resonance with the e1hh2 or e2hh1 exciton state, the transition between this state and polariton states produced by coupling of e1hh1 excitons with light becomes possible with emission of a THz photon. Also, a pillar microcavity is certainly a more appropriate structure to be fitted in still another cavity, the THz one, needed for THz lasing.

Acknowledgments — We acknowledge fruitful discussions with M. Kaliteevski, K. Kavokin, I. Shelykh and F. P. Laussy. This research is supported by the Newton International Fellowship program.

[1] D. Dragoman and M. Dragoman, *Progr. in Quant. Electronics* **28**, 1 (2004).
[2] G. Davies and E. Lienfield, *Physics World* **17**, 37 (2004).
[3] Q. Hu, B. Williams, S. Kumar, H. Callebaut, S. Kohen, and J. Reno, *Semicond. Sci. Technol.* **20**, S228 (2005).
[4] R. F. Kazarinov and R. A. Suris, *Sov. Phys. Semiconductors* **5**, 707 (1971).
[5] J. Faist, F. Capasso, D. L. Sivco, C. Sirtori, A. L. Hutchinson, and A. Y. Cho, *Science* **264**, 553 (1994).
[6] E. Normand, I. Howieson, and M. T. McCulloch, *Laser Focus*

World **43**, 90 (2007).
[7] S. De Liberato and C. Ciuti, *Phys. Rev. Lett.* **102**, 136403 (2009).
[8] K. Kavokin, M. Kaliteevski, R. Abram, A. Kavokin, S. Sharkova, and I. Shelykh, *Appl. Phys. Lett.* **97**, 201111 (2010).
[9] A. Kavokin, J. J. Baumberg, G. Malpuech, and F. P. Laussy, *Microcavities* (Oxford University Press, 2007).
[10] D. Bajoni, P. Senellart, E. Wertz, I. Sagnes, A. Miard, A. Lemaître, and J. Bloch, *Phys. Rev. Lett.* **100**, 047401 (2008).

- [11] J. Levrat, R. Butte, T. Christian, M. Glauser, E. Feltin, J.-F. Carlin, N. Grandjean, D. Read, A. V. Kavokin, and Y. Rubo, *Phys. Rev. Lett.* **104**, 166402 (2010).
- [12] E. M. Purcell, *Phys. Rev.* **69**, 681 (1946).
- [13] J.-M. Gerard and B. Gayral, *Journ. Lightwave Technol.* **17**, 2089 (1999).
- [14] Y. Todorov, I. Sagnes, I. Abram, and C. Minot, *Phys. Rev. Lett.* **99**, 223603 (2007).
- [15] M. Holland, K. Burnett, C. Gardiner, J. I. Cirac, and P. Zoller, *Phys. Rev. A* **54**, R1757 (1996).
- [16] F. P. Laussy, G. Malpuech, A. Kavokin, and P. Bigenwald, *Phys. Rev. Lett.* **93**, 016402 (2004).
- [17] E. del Valle, D. Sanvitto, A. Amo, F. P. Laussy, R. André, C. Tejedor, and L. Viña, *Phys. Rev. Lett.* **103**, 096404 (2009).
- [18] C. W. Gardiner and P. Zoller, *Phys. Rev. A* **55**, 2902 (1997).